

Toluene Dioxygenase-Catalyzed Synthesis of *cis*-Dihydrodiol Metabolites from 2-Substituted Naphthalene Substrates: Assignments of Absolute Configurations and Conformations from Circular Dichroism and Optical Rotation Measurements

Marcin Kwit,^[a] Jacek Gawronski,^{*[a]} Derek R. Boyd,^{*[b]} Narain D. Sharma,^[b] Magdalena Kaik,^[b] Rory A. More O’Ferrall,^[c] and Jaya S. Kudavalli^[c]

Abstract: *cis*-Dihydrodiol metabolites have been isolated from naphthalene and six 2-substituted naphthalene substrates. Their structures and absolute configurations have been determined by a combination of calculated (TDDFT) and experimentally based circular dichroism (CD) and optical rotation (OR) methods. The “inverse” styrene helicity rule is shown to be incorrect for the interpretation of the

CD spectra of *cis*-dihydrodiols. A striking conclusion is that CD spectra correlate directly with the helicity of the styrene chromophore: that is, the sign of the long-wavelength Cotton effect is identical with the sign of styrene tor-

sion angle, whereas the OR sign is dependent on the absolute configuration of the allylic carbon atom. The results demonstrate that a predictive model previously used for the determination of preferred regio- and stereoselectivity associated with TDO-catalyzed *cis*-dihydroxylation of substituted benzene substrates can now be successfully extended to substituted naphthalene substrates.

Keywords: absolute configuration • bacterial metabolites • circular dichroism • diols • optical rotation

Introduction

The toluene dioxygenase-catalyzed (TDO-catalyzed) dihydroxylation of mono- and disubstituted benzene substrates in bacteria has been reported to give a wide range (>200) of *cis*-dihydrodiol metabolite derivatives that have mainly been formed as single enantiomers.^[1–12] Similarly, the bacterial naphthalene dioxygenase-catalyzed (NDO-catalyzed) dihydroxylation of naphthalene and substituted naphthalenes has recently been reported to give over 25 corresponding *cis*-dihydrodiol derivatives, but in many cases neither their

enantiomeric excess (*ee*) values nor their absolute configurations have been rigorously established. The TDO-catalyzed *cis*-dihydroxylation of monosubstituted benzene *cis*-dihydrodiols (**A**) was found to be very regioselective for the 2,3-bond, giving *cis*-dihydrodiols of type **B** (Scheme 1). To date only one example of a type **C** *cis*-dihydrodiol (X=F) has been reported using the enzyme TDO.^[13a] Although no examples of type **D** *cis*-dihydrodiols have been reported with TDO as biocatalyst, one example has also been obtained using benzoate dioxygenase (BZDO). Thus using whole cells of *Alcaligenes eutrophus* (also described as *Ralstonia eutropha*) a BDZO-catalysed oxidation of benzoic acid gave a type **D** *cis*-dihydrodiol (R=CO₂H).^[13a]

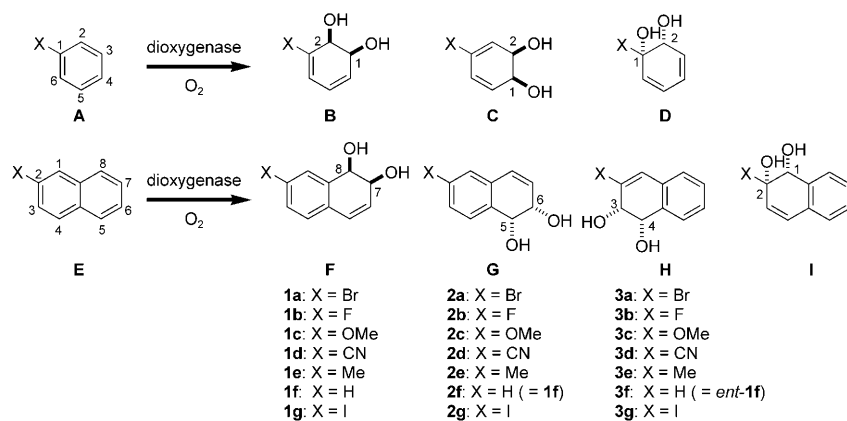
The NDO enzyme has not been reported to biotransform monosubstituted benzene substrates, with the exceptions of biphenyl **A** (X=Ph) and azabiphenyl analogues (X=pyridin-1-, -2- and -3-yl).^[13] However, a marked degree of regioselectivity was observed in bacterial NDO-catalyzed *cis*-dihydroxylation of acceptable 2-substituted naphthalene substrates (**E**), with preferential attack occurring at the 7,8-bonds to give *cis*-dihydrodiols of type **F** (X=Cl, Br, Me, Et, CO₂Me, OMe, NO₂) as major metabolites, (Scheme 1 and Table 1).^[14–18] The NDO enzyme present in a mutant strain of *Pseudomonas putida* (9816/11) was also found to catalyze

[a] Dr. M. Kwit, Prof. Dr. J. Gawronski
Grunwaldzka 6, 60 780 Poznan (Poland)
Fax: (+48) 61 829 1505

[b] Prof. Dr. D. R. Boyd, Dr. N. D. Sharma, Dr. M. Kaik
Centre for Theory and Application of Catalysis
School of Chemistry, The Queen’s University of Belfast
Belfast BT9 5AG (UK)
Fax: (+44) 909 74 687

[c] Prof. Dr. R. A. More O’Ferrall, Dr. J. S. Kudavalli
School of Chemistry and Chemical Biology
UCD Dublin 4 (Ireland)

Supporting information for this article is available on the WWW under <http://dx.doi.org/10.1002/chem.200801686>.



Scheme 1. Possible *cis*-dihydrodiol regioisomers (**B–D**, **F–I**) formed from dioxygenase-catalyzed *cis*-dihydroxylation of monosubstituted benzene (**A**) and naphthalene (**E**) substrates.

Table 1. Relative yields [%] of *cis*-dihydrodiol metabolites **F–H** obtained by TDO- and NDO-catalysed dihydroxylation of 2-substituted naphthalene substrates **E**.

X	F		G		H
	TDO (%)	NDO	TDO (%)	NDO	TDO (%)
Br	1a (33) ^[a,b]	1a ^[c,d]	2a (40) ^[a,e]	2a ^[c]	3a (27) ^[a,e]
F	1b (42) ^[a,b]		2b (20) ^[a,e]		3b (38) ^[a,f]
OMe	1c (17) ^[a,b,g]	1c (93) ^[c,d]	2c (52) ^[a,e,g]	2c (7) ^[g]	3c (31) ^[a,f,g]
CN	1d (15) ^[a,b]		2d (57) ^[a,e]		3d (28) ^[a,f]
Me	1e (60) ^[a,b,h]	1e ^[d,e,g]	2e (10) ^[a,e]		3e (30) ^[a,f]
H	1f (100) ^[a,d,i]	1f ^[d]			
I	1g (51) ^[a,b]		2g (34) ^[a,e]		3g (15) ^[a,f]

[a] Present study. [b] Mid R_f . [c] Ref. [14]. [d] Ref. [18]. [e] Low R_f . [f] High R_f . [g] Ref. [15–16]. [h] Ref. [17]. [i] Ref. [18].

cis-dihydroxylation at the 5,6-bonds of 2-methoxynaphthalene and 2-bromonaphthalene (**E**, X = OMe and Br) to give the corresponding *cis*-dihydrodiols **G** (X = OMe and Br) as very minor metabolites (<10% relative yields).^[14,15] Alternative *Pseudomonas* strains (A3 and C22) expressing a further type of NDO were also found to catalyse *cis*-dihydroxylation at the 1,2-bonds of the naphthalene rings in the carboxylic acids **E** (X = CO₂H and CH₂CO₂H) to give isolable *cis*-dihydrodiols **I** (X = CO₂H and CH₂CO₂H) as the sole metabolites.^[19]

It is noteworthy that, to date, only the TDO enzyme has been reported to catalyse *cis*-dihydroxylation at the 3,4-bonds of 2-substituted naphthalenes **E** (X = Me and OMe) to give *cis*-dihydrodiols **H** (X = Me and OMe) as minor metabolites.^[15,16] As a logical extension of our earlier studies of the combined use of experimentally obtained and calculated circular dichroism (CD) spectroscopy and optical rotation (OR) measurements in the context of assigning absolute configurations to *cis*-dihydrodiol metabolites of mono- and disubstituted benzene substrates, this study has focused on 2-substituted naphthalene substrates **E** (X = H, Me, CN, F, Br, I, OMe). The major objectives of this study were i) to extend the validity of the calculation-based and experimentally based approaches to the assignment of absolute configurations from CD and OR characteristics from monosubstituted

cis-dihydrodiols to a range of previously reported, and new, *cis*-dihydrodiols obtained from 2-substituted naphthalenes, and ii) to extend the applicability of our predictive model for assignment of the most favoured type of regioselectivity and stereoselectivity during TDO-catalyzed *cis*-dihydroxylation from substituted monocyclic arenes to their bicyclic counterparts, and also from monosubstituted and disubstituted arene rings up to trisubstituted systems.

Among the methods currently available for stereostructure (absolute configuration and conformation) assignment, methods based on the chiroptical properties of a molecule, mainly electronic circular dichroism (ECD) and optical rotation (OR), provide good alternatives to methods based on X-ray diffraction. At present, it can be useful to compare experimentally acquired data and quantum-chemical calculations of spectroscopic properties of molecules.^[20,21] As a result, information about both the conformation and the absolute configuration of a molecule (absolute stereochemistry) can be obtained. Although the absolute stereochemistry of the investigated molecule can be accurately determined by use of just one of the chiroptical methods (i.e., ECD or OR), concurrent use of more than one chiroptical method is preferred for independent assignment of molecular structures, particularly in difficult cases.^[22]

Many *ab initio* methods are now well established as indispensable partners to experimental data for prediction of chiroptical phenomena.^[23] Of these, those based on time-dependent density functional theory (TD-DFT) are the most frequently used. Among the many functionals available, the B3LYP hybrid functional in conjunction with the basis sets varying from the relatively small (that is, 6-31G(D)) to the very large (that is, Aug-CC-pVXZ) appear to have the broadest applicability.^[24,25] Although the B3LYP functional is the most frequently used for calculations of many molecular properties, including some ECD and OR calculations, it can produce unsatisfactory results in calculations of some properties, such as those that depend on long- and medium-range noncovalent interactions and in the case of transition-metal chemistry.^[26,27] In recent years, the development of new functional forms, and their validation against diverse databases, have yielded powerful new density functionals of broad applicability to many areas of chemistry.^[28] Among these, hybrid density functionals, including a non-local correlation effect, have given promising results in cases of calculations of molecular properties both in the ground and in excited states.^[29] The virtual-orbital-dependent B2PLYP hybrid functional, recently developed by Grimme and Schwabe, is based on a mixing of standard generalized gra-

dient approximations (GGAs), which have been used for exchange by Becke (B) and for correlation by Lee, Yang and Parr (LYP) with Hartree–Fock (HF) exchange and a perturbative second-order correlation part (PT2) that is obtained from Kohn–Sham (GGA) orbitals and eigenvalues.^[30] Extensive testing has recently demonstrated the outstanding accuracy of this approach for various ground-state problems in general chemistry applications.^[31] In our computations of chiroptical properties of naphthalene *cis*-dihydrodiols, we used the B2PLYP hybrid functional in conjunction with a 6-311++G(2D,2P) basis set for ECD calculations, and a B3LYP/6-311++G(2D,2P) method for OR calculations.

Results and Discussion

TDO-catalysed *cis*-dihydroxylations of naphthalene **1f and the 2-substituted naphthalenes **1a–e** and **1g**:** The UV4 mutant strain of *Pseudomonas putida* has been extensively used as a source of TDO, and the majority of *cis*-dihydrodiol metabolites from mono- and disubstituted benzene substrates that have to date been isolated, identified and stereochemically assigned are from this strain.^[1–12] Bacterial NDO uses naphthalene (**E**, X = H) as its natural substrate and it is evident that 2-substituted naphthalene derivatives **E** (X = Me, Et, CO₂Me, Cl, Br, OMe, NO₂) are also substrates for this enzyme, giving mainly bioproducts of type **F**. Literature reports^[16,19] of the TDO-catalyzed *cis*-dihydroxylation of the 2-substituted naphthalene substrates **E** (X = Me, OMe) by Hudlicky et al., however, suggested that this enzyme could also produce the two other *cis*-dihydrodiol regioisomers of types **G** and **H** (Table 1).

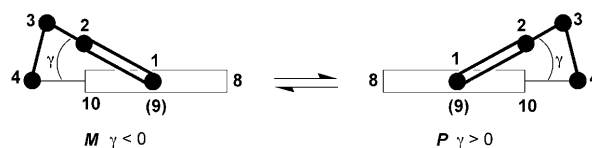
With whole cells of *P. putida* UV4 (expressing TDO), biotransformations of naphthalene and six substituted naphthalenes (**E**, X = H, Br, F, OMe, CN, Me, I) yielded a total of nineteen *cis*-dihydrodiols of i) type **F** [**1a** (X = Br), **1b** (X = F), **1c** (X = OMe), **1e** (X = Me), **2d** (X = CN), **1f** (X = H) and **1g** (X = I)], ii) type **G** [**2a** (X = Br), **2b** (X = F), **2c** (X = OMe), **2d** (X = CN), **2e** (X = Me) and **2g** (X = I)], and iii) type **H** [**3a** (X = Br), **3b** (X = F), **3c** (X = OMe), **3d** (X = CN), **3e** (X = Me), **3g** (X = I)]. The majority of these *cis*-dihydrodiols had not previously been reported as metabolites.

Mixtures of the *cis*-dihydrodiol regioisomers were generally separated by preparative TLC. While individual samples of compounds **1e**, **2d**, **3d** and **3e** were obtained after chromatography and recrystallisation, unfortunately the corresponding *cis*-dihydrodiol isomers **1d** and **2e** could not be isolated as pure compounds by these methods. A single-step chemical substitution of the iodine atom in compound **1g** with a CN group, however, did yield a pure sample of *cis*-dihydrodiol **1d**. While it was possible to estimate the relative proportion of metabolite **2e** from its NMR spectrum, neither OR nor experimental ECD data were recorded (for analytical data for *cis*-dihydrodiols see the Supporting Information).

The regiochemistries and absolute stereochemistries of seven of the nineteen *cis*-dihydrodiol metabolites (**1a**, **1c**,

1e, **1f**, **2c**, **3a**, **3c**) had been unequivocally determined earlier.^[14–18] NMR analysis (NOE, HMBC, coupling constants) and aromatisation and identification of the known phenolic derivatives were used to ascertain the regiochemistries of all of the *cis*-dihydrodiols isolated during the current study. The enantiomeric excess (*ee*) values for all *cis*-dihydrodiols were found to be >98% through the formation of chiral boronate derivatives by methods described earlier.^[32–35] The absolute configurations were all assigned by a method of comparison of calculated and experimentally measured CD spectra and OR.^[32–35]

Conformational analysis of *cis*-dihydrodiols **1a–f, **2a–e** and **3a–e**:** In order to obtain reliable results from CD and OR calculations, we first carried out calculations for low-energy conformers of *cis*-dihydrodiols by the previously described protocol.^[32–35] The calculated structures of the low-energy conformers were optimized by use of the B3LYP functional and the enhanced basis set 6-311++G(D,P). Up to five conformers within the 2.0 kcal mol^{−1} energy window were obtained for each *cis*-dihydrodiol. These conformers belong to two families, distinguished by their senses of helicity (*M* or *P*) of the styrene (1,2-dihydronaphthalene) chromophore (Scheme 2). Calculated styrene skew angles γ (C2–C1–C9–C10) of the *cis*-dihydrodiol metabolites (see the Supporting Information) are all within the narrow ranges of 10.3 to 12.5° (for *P*) and −10.6 to −12.8° (for *M*).

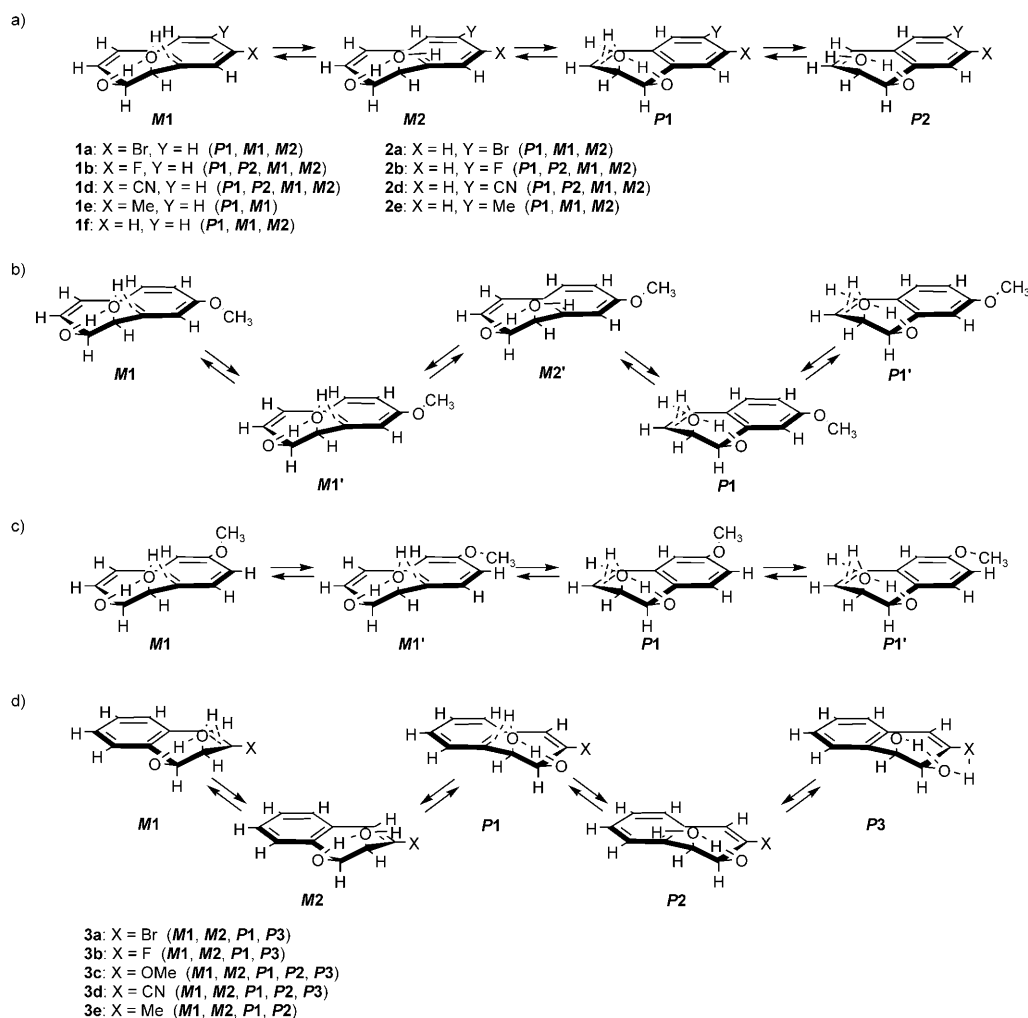


Scheme 2. *M* and *P* enantiomers of the styrene chromophore in 1,2-dihydronaphthalenes.

The presence of the 3,4-*cis*-OH systems in the *cis*-dihydrodiols facilitates the preferred conformations resulting from their rotation and hydrogen bonding. A detailed list of the types of thermally accessible conformers for each *cis*-dihydrodiol is given in Scheme 3.

As previously noted for *cis*-cyclohexa-3,5-diene-1,2-diols^[32–35] all conformers feature structures stabilized by intramolecular OH...O hydrogen bonds. In the **M1** and **P1** conformers, torsion angles α (H–C3–O–H) and β (H–C4–O–H) are *anti*, whereas in the case of the **M2** and **P2** conformers one of these torsion angles is *anti* and the other is *syn* (Scheme 3a). Calculated values of angles α and β (see the Supporting Information) are within the ranges of $\pm(153$ to $165^\circ)$ for *anti* and $\pm(50$ to $91^\circ)$ for *syn*. These angles are positive for **M1** and **M2** conformers and negative for **P1** and **P2** conformers.

The presence of a heteroatom substituent (Br, F) or a group bearing a heteroatom (OMe, CN) in a position vicinal to a hydroxy group in each of **3a–d** introduces an additional

Scheme 3. Diastereomeric *P* and *M* conformers of *cis*-dihydrodiols: a) **1**, **2**; b) **1c**; c) **2c**; d) **3**.

possibility for conformer stabilisation through an OH...heteroatom hydrogen bond. In each of these conformers (**P3**) the pseudoaxial hydroxy group at C4 is a donor for the hydroxy group at C3, and this in turn is a hydrogen bond donor to a heteroatom at C2 (Scheme 3d). In **P3** conformers both torsion angles α and β are (+)-*syn*.

The presence of a methoxy substituent at C2 in dihydrodiol derivatives **1c** and **2c** makes the number of accessible conformers even larger, due to rotation of this substituent around the C2–O bond. The methyl group can be *syn* to either of the hydrogen atoms at vicinal carbon atoms of the aromatic ring (**M1**, **M1'**, **P1**, **P1'** in Scheme 3b and c). The effect of the vicinal hydroxy group in **3c** (and to some extent in **1c**, conformer **M2'**) forces the methoxy group away from the hydrogen of the hydroxy group and reduces the number of possible conformers due to rotation of the methoxy group.

The calculated populations of the conformers are given in Table 2.

In the cases of dihydrodiols **1a–f** and **2a–e**, the lowest-energy conformer in each case is of the **P1** (or **P1'**) type, in

which the equatorial hydroxy group at C4 donates a hydrogen bond to the axial oxygen atom at C3 and the hydrogen atom of this hydroxy group engages in the formation of a OH... π hydrogen bond. The population of **P1+P1'** conformers is at least 60% (ΔE calculation), except in the case of **2c**, for which approximately equal populations of **M1+M1'** and **P1+P1'** conformers were calculated. An equatorial O–H...axial OH... π hydrogen bond pattern is apparently a stabilising factor in all conformers of **M1**, **M2**, **P1** and **P2** type.

In the cases of dihydrodiols **3a–e**, the more stable conformers are of *M* helicity, evidently reflecting stronger C3 axial OH... π bonding with the C2-substituted double bond (**M1**) or the effect of stabilising dipole–dipole interaction between the vicinal O–H and C–X bonds (**M2**). Clear-cut evidence for the effect of the nature of the C2 substituent on the stability of *M* conformers is provided in dihydrodiols **3d** and **3e**. Whereas the **M2** conformer is the most stable for the cyano-substituted dihydrodiol **3d**, it is the least stable in the case of the methyl-substituted dihydrodiol **3e** (Scheme 3 and Table 2). This situation is reminiscent of the conformational preferences of *cis*-dihydrodiol metabolites of

Table 2. Calculated B3LYP/6-311++G(D,P) relative energies (ΔE , ΔG) and populations for low-energy conformers of **1a-f**, **2a-e** and **3a-e** (values in italics indicate the lowest energy conformation).

Diol	Conformer	ΔE [kcal mol ⁻¹]	Population [%]	ΔG [kcal mol ⁻¹]	Population [%]
1a	<i>M1</i>	0.94	16	0.62	27
	<i>M2</i>	1.70	4	1.15	10
	<i>P1</i>	0.00	80	0.00	63
1b	<i>M1</i>	1.19	13	0.93	13
	<i>M2</i>	2.06	–	1.51	5
	<i>P1</i>	0.00	83	0.00	65
	<i>P2</i>	1.57	4	0.76	17
1c	<i>M1</i>	1.32	6	0.92	10
	<i>M1'</i>	1.34	6	0.94	9
	<i>M2'</i>	2.22	–	1.43	4
	<i>P1</i>	0.00	59	0.00	48
	<i>P1'</i>	0.40	29	0.30	29
1d	<i>M1</i>	0.90	15	1.99	3
	<i>M2</i>	1.42	7	2.30	–
	<i>P1</i>	0.00	71	0.00	97
	<i>P2</i>	1.31	7	2.15	–
1e	<i>M1</i>	0.66	24	0.84	19
	<i>P1</i>	0.00	76	0.00	81
1f	<i>M1</i>	0.60	25	0.33	31
	<i>M2</i>	1.51	5	0.83	14
	<i>P1</i>	0.00	70	0.00	55
2a	<i>M1</i>	0.70	22	0.43	28
	<i>M2</i>	1.55	5	0.83	14
	<i>P1</i>	0.00	73	0.00	58
2b	<i>M1</i>	0.47	28	0.25	30
	<i>M2</i>	1.34	6	0.64	16
	<i>P1</i>	0.00	62	0.00	46
	<i>P2</i>	1.62	4	1.01	8
2c	<i>M1</i>	0.26	21	0.15	25
	<i>M1'</i>	0.12	26	0.00	33
	<i>P1</i>	0.25	21	0.42	16
	<i>P1'</i>	0.00	32	0.13	26
2d	<i>M1</i>	1.22	10	0.97	12
	<i>M2</i>	1.95	2	1.39	6
	<i>P1</i>	0.00	79	0.00	65
	<i>P2</i>	1.29	9	0.79	17
2e	<i>M1</i>	0.41	31	1.42	5
	<i>M2</i>	1.32	6	0.32	35
	<i>P1</i>	0.00	63	0.00	60
3a	<i>M1</i>	0.00	54	0.01	43
	<i>M2</i>	0.26	34	0.00	43
	<i>P1</i>	1.22	7	1.04	7
	<i>P3</i>	1.32	5	1.11	7
3b	<i>M1</i>	0.00	60	0.00	48
	<i>M2</i>	0.48	26	0.16	37
	<i>P1</i>	1.17	8	0.99	9
	<i>P3</i>	1.42	6	1.23	6
3c	<i>M1</i>	0.00	48	0.00	42
	<i>M2</i>	0.43	23	0.21	29
	<i>P1</i>	1.68	2	1.49	4
	<i>P3</i>	0.34	27	0.30	25
3d	<i>M1</i>	0.01	42	0.27	30
	<i>M2</i>	0.00	42	0.00	48
	<i>P1</i>	1.08	6	1.11	7
	<i>P2</i>	1.59	3	1.37	5
	<i>P3</i>	1.01	7	0.94	10
3e	<i>M1</i>	0.00	68	0.00	52
	<i>M2</i>	2.26	0	1.64	3
	<i>P1</i>	0.54	27	0.32	31
	<i>P2</i>	1.54	5	0.75	14

type **B** (Scheme 1), for which the **M2** conformer is of the lowest energy when X is a heteroatom substituent.^[32]

Absolute configurations of *cis*-dihydrodiols from studies of circular dichroism and optical rotation: Dihydrodiols **1a-f**, **2a-e** and **3a-e** each contain the styrene chromophore embedded in the 1,2-dihydronaphthalene framework. Such a structural feature is frequently encountered in other classes of natural^[36] and synthetic^[37] compounds. The characteristic electronic π - π^* transition involving the orbitals of both the benzene and the ethylene part of the styrene chromophore is located in the electronic spectra at ca. 260–270 nm; for 1,2-dihydronaphthalene in hexane solution this transition appears at 258 nm ($\epsilon=9070$).^[38] Almost forty years ago, Crabbé postulated an empirical helicity rule for the styrene chromophore, which correlates the sign of the 260–270 nm transition Cotton effect with the helicity: that is, the sign of the torsion angle γ (Scheme 2). According to this rule, an *M* helical styrene chromophore ($\gamma < 0$) is characterized by a positive Cotton effect, and conversely, a negative Cotton effect is associated with *P* helicity ($\gamma > 0$) of the styrene chromophore.^[39] However, only a limited number of styrene chromophore-containing compounds were used in these empirical correlations, so the general applicability of the rule remains unknown. In this study we used the calculated structures of low-energy conformers of *cis*-dihydrodiols (Table 2) to calculate their CD spectra by the TDDFT method at the B2PLYP/6-311++G(2D,2P) level. The computed energies (λ_{\max}), oscillator strengths (*f*) and rotatory strengths (*R*) for the styrene long-wavelength π - π^* transition are collected in Table 3.

The effect of a substituent X on the calculated λ_{\max} value of the 260–270 nm transition is distinctive. Relative to the unsubstituted dihydrodiol **1f**, significant red shifts of λ_{\max} are observed for cyano-substituted dihydrodiols **1d**, **2d** and **3d**. In the case of **3d**, with the cyano group attached to the ethylene group, this shift exceeds 20 nm. Substituent effects are also seen in the increase in oscillator strength of the transition.

In the cases of **1d** and **3d** there are twofold increases in *f* relative to the corresponding value for **1f**, but for **2d** a twofold decrease in *f* is calculated. These changes can be accounted for by a change in the conjugation pattern of the π electron system in the isomers of the cyano-substituted *cis*-dihydrodiols. The corresponding experimentally determined values ϵ (λ_{\max}) available for *cis*-dihydrodiols (in acetonitrile solution) are as follows: $\epsilon = 8500$ (268 nm) for unsubstituted **1f**, $\epsilon = 1600$ for cyano-substituted **2d** (293 nm), and $\epsilon = 18200$ (290 nm) for **3d**. A similar red shift (over 20 nm), together with either a decrease in ϵ (for **2d**) or an increase in ϵ (for **3d**) due to the CN substituent is therefore observed experimentally, providing a good check of the reliability of the method of calculation used in this study. A further test of the quality of the calculations is presented in Figure 1.

Excellent agreement between the experimentally measured and calculated UV spectra of the bromine- and fluorine-substituted dihydrodiols **1a/2a/3a** and **1b/2b/3b** was

Table 3. Calculated [B2PLYP/6-311++G(2D,2P) level] excitation energies (λ_{\max}), oscillator strengths (f) and rotatory strengths (R) for the lowest-energy electronic transitions for low-energy conformers of **1a–f**, **2a–e** and **3a–e**.

Diol	Conformer	λ_{\max} [nm]	f	R [10^{-40} ergesu cm Gauss $^{-1}$]
1a	M1	267	0.244	−0.830
	M2	269	0.250	1.151
	P1	266	0.313	7.312
1b	M1	263	0.116	−15.506
	M2	264	0.117	−17.285
	P1	259	0.182	31.505
1c	P2	262	0.204	31.231
	M1	276	0.150	−7.364
	M1'	270	0.161	−0.176
1d	M2'	270	0.157	−0.855
	P1	274	0.222	40.680
	P1'	268	0.281	14.762
1e	M1	273	0.372	5.010
	M2	276	0.375	9.306
	P1	271	0.373	2.488
1f	P2	273	0.378	3.170
	M1	264	0.192	−1.479
	P1	263	0.258	19.519
2a	M1	260	0.171	−15.426
	M2	262	0.175	−15.896
	P1	259	0.199	27.172
2b	M1	261	0.138	−21.695
	M2	263	0.146	−21.091
	P1	262	0.128	20.891
2c	M1	258	0.196	−16.570
	M2	260	0.202	−15.985
	P1	261	0.173	15.203
2d	P2	264	0.184	17.896
	M1	267	0.138	−19.104
	M1'	259	0.112	−17.447
2e	P1	275	0.120	14.270
	P1'	269	0.086	11.434
	M1	271	0.074	−18.251
3a	M2	274	0.080	−20.378
	P1	263	0.099	44.058
	P2	264	0.113	43.597
3b	M1	259	0.159	−20.249
	M2	261	0.166	−20.345
	P1	263	0.161	19.031
3c	M1	270	0.314	−12.965
	M2	269	0.322	−17.756
	P1	270	0.304	19.722
3d	P3	266	0.325	10.940
	M1	259	0.167	−37.052
	M2	259	0.176	−38.441
3e	P1	262	0.134	23.507
	P3	260	0.113	11.266
	M1	265	0.223	−23.830
3f	M2	264	0.229	−30.961
	P1	271	0.176	21.981
	P3	264	0.199	10.898
3g	M1	283	0.389	−0.068
	M2	285	0.399	0.865
	P1	279	0.409	−4.254
3h	P2	281	0.405	−2.819
	P3	280	0.442	−12.409
	M1	261	0.245	−25.858
3i	M2	263	0.252	−27.502
	P1	264	0.208	31.970
	P2	267	0.220	27.959

obtained, including a red shift of the long-wavelength λ_{\max} of the bromine-substituted dihydrodiol **3a** in relation to its isomers **1a** and **2a** and a small effect of the fluorine substituent on the absorption spectra of **1b**, **2b** and **3b**.

The calculated rotatory strengths (R) of individual conformers of *cis*-dihydrodiols (Table 3) in general correlate well with the sense of helicity of the styrene chromophore, except for the cases in which the calculated rotatory strengths are low. Thus, a negative (positive) rotatory strength is associated with *M* (*P*) helicity of the styrene chromophore, which is in contradiction to the empirical rule postulated by Crabbé. Exceptions include the **M2** conformers of the bromo-substituted dihydrodiols **1a** or **3d**, the **M1** and **M2** conformers of the cyano-substituted dihydrodiol **1d** and the **P1** and **P2** conformers of compound **3d** (**2d** behaved unexceptionally). Note, however, that the cyano substituent is a special case. Previously we have shown^[32] that the signs of the long-wavelength π - π^* Cotton effects of cyclohexa-1,3-dienes change upon introduction of a cyano substituent into the diene π electron system.

Calculated Boltzmann-averaged and experimentally measured CD spectra of *cis*-dihydrodiols are shown in Figure 2. In general, good (although not perfect) agreement between the experimentally measured spectra and those calculated for the assumed absolute configurations shown in Scheme 1 is observed not only for the longer-wavelength styrene chromophore transition Cotton effect but also for the shorter-wavelength CD bands. Contrary to the very good agreement of calculated and experimentally measured UV spectra (Figure 1), less perfect fits of the corresponding CD spectra can be expected, as the experimentally measured CD spectra are highly dependent on conformational equilibrium and the environment (solvent effects).

As no pure sample of metabolite **2e** was isolated, no experimentally measured CD spectrum was available for comparison with the calculated CD spectrum.

We also note that the shapes of the experimentally measured CD spectra of the iodine-substituted dihydrodiols **1g**, **2g** and **3g** (see the Supporting Information) are similar to those of the bromine-substituted analogues **1a**, **2a** and **3a** (except for the long-wavelength part of the spectrum of **1g**). This establishes the absolute configurations of the iodine-substituted dihydrodiols **1g** (*7S,8R*), **2g** (*5R,6S*) and **3g** (*3R,4S*). Chemical substitution of the iodine atom in compound **1g** [Bu_3SnCN , $[\text{Pd}(\text{PPh}_3)_4]$, Et_3N in THF] to yield a pure sample of *cis*-dihydrodiol **1d** provides further confirmation of the (*7S,8R*) configuration.

Further strong evidence of the assigned absolute configurations for dihydrodiols **1a–f**, **2a–e** and **3a–e** was obtained from the calculation of their optical rotations. The calculations were carried out for each low-energy conformer and for the Boltzmann-averaged (ΔE) mixtures of conformers at the B3LYP/6-311++G(2D,2P) level. In order to achieve high reliability in the calculations we computed the optical rotation values at four different wavelengths (589, 578, 546, 436 nm) and compared the averaged data with the experimental measurements in methanol (Table 4).

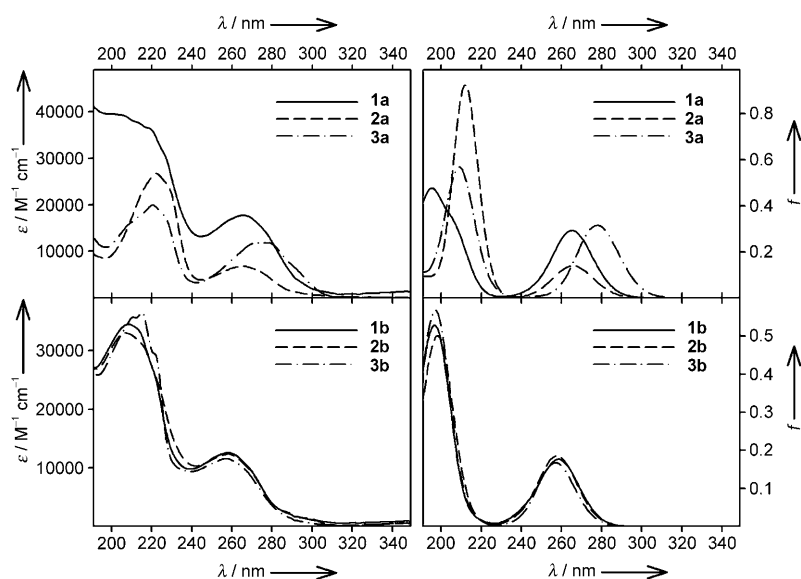


Figure 1. Experimentally measured (in acetonitrile solution, left-hand panels) and Boltzmann-averaged calculated [B2PLYP/6-311++G(2D,2P) level, right-hand panels] UV spectra of *cis*-diols **1a**, **2a**, **3a**, **1b**, **2b** and **3b**. All calculated spectra were wavelength-corrected to match experimentally measured long-wavelength λ_{max} values.

In general, the calculated and experimentally measured $[\alpha]_{\lambda}$ values are large, which makes the comparison highly reliable. We observe excellent agreement between the experimentally measured and the calculated optical rotation data. Therefore, in combination with the CD data discussed above, the absolute configurations of the *cis*-dihydrodiols are assigned unequivocally. As noted previously, no experimental data are available for metabolite **2e**.

A more detailed analysis of the calculated OR for individual conformers of *cis*-dihydrodiols (Table 4) reveals that, unlike in the case of the CD spectra, the sign of optical rotation does not correlate directly with the helicity of the styrene chromophore. In the series **1a–f** and **2a–e**, **M1** and **M2** conformers display $[\alpha]_{\text{D}}$ values of the same sign (positive) as the **P1** and **P2** conformers. On the other hand, **P** conformers of **3b** and **3d** have negative OR values. In the cases of the **M2** conformers of dihydrodiols **1b**, **1f**, **2b**, **2d** and **2e** and of the **P1** conformers of **3b** and **3c**, the calculated $[\alpha]$ values are low and the optical rotation changes sign as the wavelength changes. A striking finding is that the sign of OR can be directly correlated with the helicity of the allylic bond system, consisting of C5=C6–C7–O in **1a–f** (*P* helicity), C8=C7–C6–O in **2a–e** (*P* helicity) and C1=C2–C3–O in **3a–e** (*M* helicity). Positive optical rotations at the D line (589 nm) are calculated for all (**M** or **P**) styrene conformers in the first two dihydrodiol series (**1**, **2**), and negative $[\alpha]_{\text{D}}$ values (or weakly positive values) were obtained for the conformers of the last series (**3**). The helicity of the allylic bond system can be directly used for the assignment of absolute configuration at the allylic position: that is, *7S* in **1**, *6S* in **2**, *3S* in **3a–c** and *3R* in **3d** and **3e**. This can be explained in a simple way. Both the equatorial and the axial allylic C–O bonds form a *P* helical system with the C=C bond in all con-

formers (**P** or **M**) of dihydrodiol molecules **1** and **2**, while an *M* helical arrangement is found in **3**. Whereas an axial allylic C–O bond contributes more strongly to optical rotation than an equatorial one, their contributions are of the same sign and are due to a series of electronic transitions occurring at shorter wavelengths (below 250 nm, see the Supporting Information) of the naphthalene *cis*-dihydrodiol molecules. On the other hand, a long-wavelength (above 250 nm) Cotton effect in the CD spectra is due to a single electronic transition that does not involve orbitals of the oxygen atom and therefore is sensitive to non-planarity of the styrene chromophore. We conclude that comparison of the measured and calculated optical

rotations is the most reliable and direct method for the assignment of absolute configurations of these naphthalene *cis*-dihydrodiols.

Conclusions

We have developed a computational model to predict the absolute configurations and conformations of (2-substituted) naphthalene *cis*-dihydrodiol metabolites containing the styrene chromophore. Contrary to predictions based on the previous *inverse* empirical correlation (Crabbé) between the sign of the styrene torsion angle and the sign of its long-wavelength Cotton effect, the present study shows that this relationship is simple and direct: that is, a positive long-wavelength Cotton effect is associated with a positive sign for the styrene torsion angle. The absolute configuration at the allylic carbon atom of a naphthalene *cis*-dihydrodiol can be unequivocally deduced from the sign of the OR at the D line (589 nm). Thus, positive ORs are associated with *7S* configurations in *cis*-dihydrodiols **1** and *6S* configurations in *cis*-dihydrodiols **2**, whereas negative ORs of *cis*-dihydrodiols **3** are due to absolute configurations at C3 as shown in Scheme 1 (*R/S* descriptors depending here on the nature of the substituent at C2). We note that the success of the ECD calculations is due to application of the B2PLYP functional of Schwabe and Grimme. The absolute configurations obtained were all as anticipated for *cis*-dihydrodiols of types **F** and **G**: that is, benzylic *R*. Earlier work by Hudlicky et al.^[15] had indicated that the *cis*-dihydrodiol (**3c**) had a benzylic *S* configuration, whereas no unequivocal stereochemical assignment was provided for compound **3e**.^[16] These CD studies of compounds **3a–e**, have shown unequivocally that all

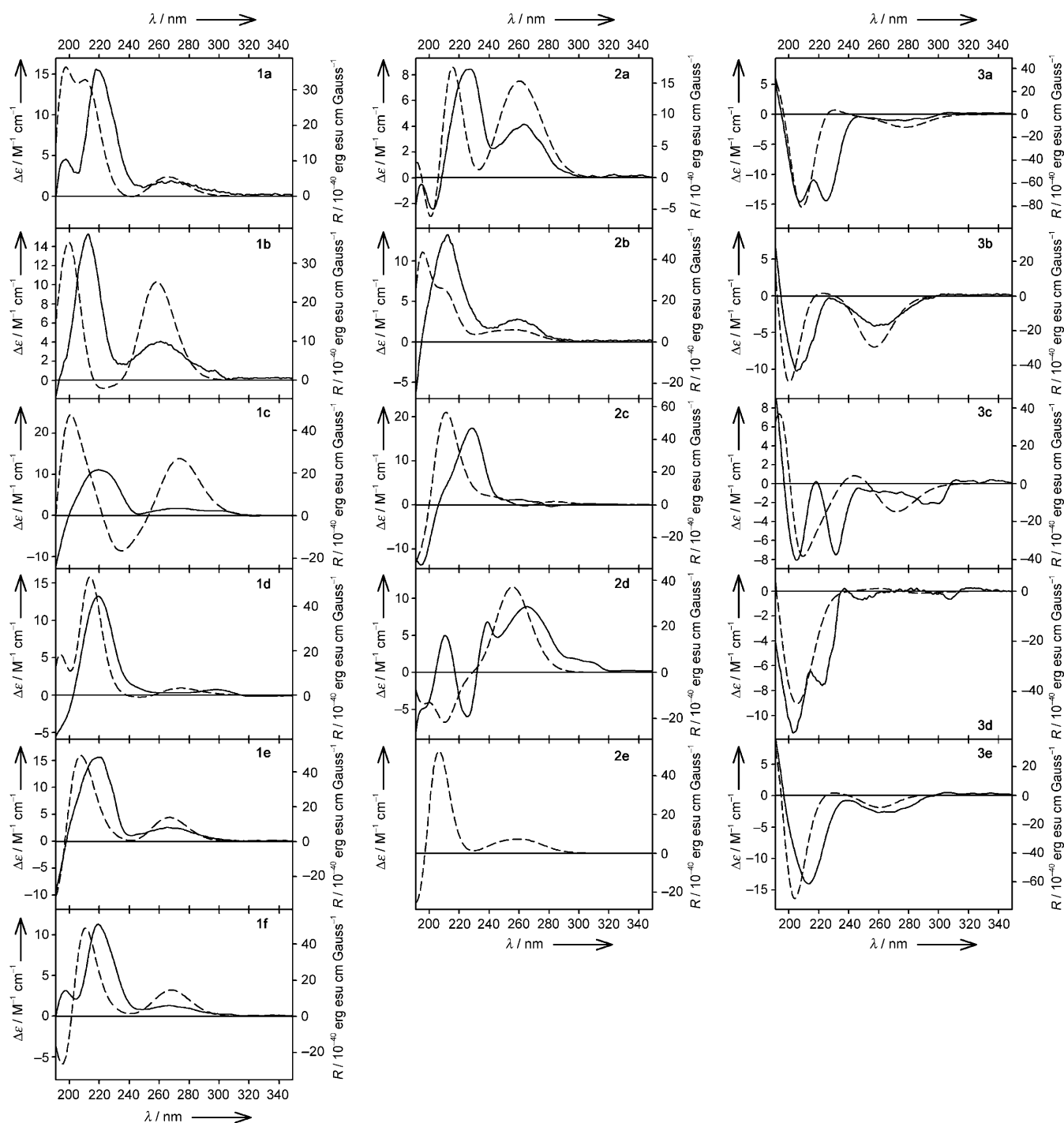


Figure 2. Experimentally measured (in acetonitrile solution, solid lines) and Boltzmann-averaged calculated [B2PLYP/6-311++G(2D,2P) level, dashed lines] CD spectra of *cis*-diols **1a-f**, **2a-e** and **3a-e**. Rotatory strengths (R) were calculated in dipole-velocity representation. All calculated spectra were wavelength-corrected to match experimentally determined long-wavelength UV λ_{max} values. No experimental data are available for **2e**.

metabolites of type **H** (including compound **3e**) resulting from TDO-catalyzed *cis*-dihydroxylation of the corresponding 2-substituted naphthalenes **E** have benzylic *S* configurations.

From these CD studies it is now possible to extend the validity of an earlier predictive model^[32–34] for the preferred regio- and stereochemistry of TDO-catalyzed *cis*-dihydroxy-

lation of monosubstituted (**A**→**B**) and *ortho*-disubstituted benzene substrates (**E'**→**F'**) to the bicyclic arene series. *cis*-Dihydrodiols of type **F** and **G** thus have the same benzylic *R* configurations as those of type **F'**, while those of type **H** have the same benzylic *S* configurations as found at C-1 in *cis*-dihydrodiols of type **B**. The *cis*-dihydroxylation of the substituted ring in the bicyclic arenes of type **E** can also be

Table 4. Specific optical rotations—both calculated at the B3LYP/6-311++G(2D,2P) level and measured—for *cis*-dihydrodiols **1a–f**, **2a–e** and **3a–e**.

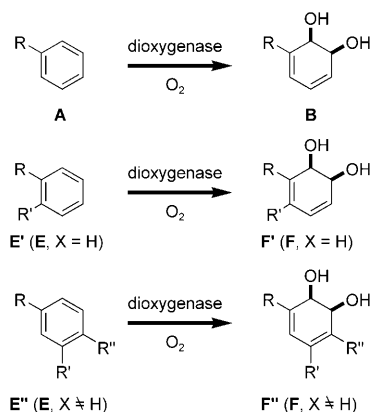
Diol	Conformer	Calculated optical rotations				Measured optical rotations ^[a]			
		589 nm	578 nm	546 nm	436 nm	589 nm	578 nm	546 nm	436 nm
1a	<i>M1</i>	+174	+233	+271	+521				
	<i>M2</i>	+93	+110	+125	+216				
	<i>P1</i>	+197	+261	+302	+575				
	ΔE Boltzmann-averaged	+189	+250	+290	+552	+240	+245	+284	+534
1b	<i>M1</i>	+134	+163	+185	+312				
	<i>M2</i>	+10	-24	-35	-149				
	<i>P1</i>	+242	+349	+410	+848				
	<i>P2</i>	+315	+449	+526	+1083				
ΔE Boltzmann-averaged	+237	+337	+395	+809	+236	+240	+279	+539	
1c	<i>M1</i>	+178	+227	+261	+472				
	<i>M1'</i>	+221	+307	+358	+711				
	<i>M2'</i>	+119	+151	+174	+323				
	<i>P1</i>	+189	+261	+305	+611				
ΔE Boltzmann-averaged	+319	+476	+562	+1229					
1d	<i>M1</i>	+267	+389	+457	+973	+276	+290	+336	+656
	<i>M2</i>	+239	+334	+390	+787				
	<i>M1</i>	+138	+184	+214	+424				
	<i>P1</i>	+238	+312	+361	+678				
ΔE Boltzmann-averaged	+310	+406	+469	+890					
1e	<i>M1</i>	+215	+302	+353	+714	+216	+228	+263	+496
	<i>M1</i>	+205	+274	+318	+603				
	<i>P1</i>	+276	+385	+449	+903				
	ΔE Boltzmann-averaged	+259	+358	+417	+831	+236	+243	+281	+533
1f	<i>M1</i>	+149	+182	+207	+355				
	<i>M2</i>	+7	-31	-42	-165				
	<i>P1</i>	+290	+416	+488	+998				
	ΔE Boltzmann-averaged	+241	+335	+391	+779	+235	+247	+287	+540
2a	<i>M1</i>	+141	+178	+205	+362				
	<i>M2</i>	+50	+39	+40	+13				
	<i>P1</i>	+134	+203	+240	+519				
	ΔE Boltzmann-averaged	+131	+189	+222	+459	+141	+143	+159	+289
2b	<i>M1</i>	+136	+167	+191	+329				
	<i>M2</i>	+14	-16	-25	-121				
	<i>P1</i>	+234	+334	+392	+798				
	<i>P2</i>	+295	+422	+495	+1015				
ΔE Boltzmann-averaged	+196	+270	+315	+620	+202	+213	+247	+469	
2c	<i>M1</i>	+148	+177	+201	+324				
	<i>M1'</i>	+173	+216	+248	+428				
	<i>P1</i>	+167	+270	+322	+735				
	<i>P1'</i>	+254	+374	+440	+930				
ΔE Boltzmann-averaged	+192	+270	+315	+631	+190	+202	+234	+447	
2d	<i>M1</i>	+168	+208	+237	+400				
	<i>M2</i>	+36	+3	-5	-124				
	<i>P1</i>	+192	+296	+351	+773				
	<i>P2</i>	+251	+375	+442	+952				
ΔE Boltzmann-averaged	+192	+288	+341	+734	+197	+205	+240	+488	
2e	<i>M1</i>	+170	+211	+241	+417				
	<i>M2</i>	+39	+14	+10	-65				
	<i>P1</i>	+225	+330	+388	+813				
	ΔE Boltzmann-averaged	+197	+274	+288	+638				
3a	<i>M1</i>	-126	-184	-216	-440				
	<i>M2</i>	-218	-309	-361	-727				
	<i>P1</i>	+9	+25	+33	+112				
	<i>P3</i>	+3	+12	+16	+53				
ΔE Boltzmann-averaged	-141	-202	-236	-474	-156	-171	-198	-384	
3b	<i>M1</i>	-256	-379	-447	-941				
	<i>M2</i>	-342	-494	-580	-1196				
	<i>P1</i>	-37	-15	-11	+59				
	<i>P3</i>	-49	-43	-46	-40				
ΔE Boltzmann-averaged	-248	-360	-423	-872	-188	-191	-221	-428	
3c	<i>M1</i>	-179	-257	-302	-627				
	<i>M2</i>	-309	-438	-513	-1049				
	<i>P1</i>	-15	+7	+14	+111				
	<i>P3</i>	-42	-44	-48	-57				
ΔE Boltzmann-averaged	-169	-236	-276	-555	-183	-190	-217	-421	

Table 4. (Continued)

Diol	Conformer	Calculated optical rotations				Measured optical rotations ^[a]			
		589 nm	578 nm	546 nm	436 nm	589 nm	578 nm	546 nm	436 nm
3d	M1	-81	-93	-104	-146				
	M2	-143	-174	-198	-329				
	P1	-134	-212	-252	-557				
	P2	-25	-44	-53	-125				
	P3	-158	-249	-296	-661				
ΔE Boltzmann-averaged		-114	-144	-164	-283	-115	-124	-144	-280
3e	M1	-223	-327	-384	-800				
	M2	-308	-439	-515	-1052				
	P1	+5	+44	+58	+207				
	P2	+91	+175	+212	+530				
ΔE Boltzmann-averaged		-146	-202	-235	-462	-192	-196	-227	-443

[a] in MeOH.

considered equivalent to that of trisubstituted monocyclic arenes **E''**, so the validity of the predictive model can be further extended (Scheme 4).



Scheme 4. Preferred TDO-catalyzed *cis*-dihydroxylation products (**B**, **F'**, **F''**) obtained from monosubstituted benzene (**A**) and naphthalene (**E'** and **E''**) substrates.

Experimental Section

General information: ¹H NMR and ¹³C NMR spectra were recorded at 300 MHz (Bruker Avance DPX-500) and at 500 MHz (Bruker Avance DRX-500) in CDCl₃ unless stated otherwise. Chemical shifts (δ) are reported in ppm relative to SiMe₄, and coupling constants (J) are given in Hz. CD and UV spectra were measured on JASCO 720 or 810 spectropolarimeters. Mass spectra were recorded at 70 eV on a VG Autospec mass spectrometer with a heated inlet system. Accurate molecular weights were determined by the peak matching method with perfluorokerosene as standard. FT-IR spectra were taken as KBr pellets on a Perkin-Elmer spectrometer. Chiral stationary phase HPLC was carried out with a Shimadzu LC-6A liquid chromatograph connected to a Hewlett Packard diode array detector. The 2-substituted naphthalene substrates were obtained commercially except for 2-iodonaphthalene, which was synthesized by a literature procedure.

Shake flask biotransformations (1–8 g) were carried out with *Pseudomonas putida* UV4 under the reported conditions.^[13,33,41] The mixtures of *cis*-dihydrodiol isomers (**1a–g**, **2a–f**, **2g**, **3a–e**, **g**) formed from biotransformation of each of the 2-substituted naphthalene substrates were separated by flash chromatography on silica gel with elution either with hexane and an increasing proportion of EtOAc or by multi-elution PLC with hexane/ethyl acetate (80:20)→(50:50). The elution sequence for *cis*-dihydro-

drodiol isomers is shown in Table 1 and the relative R_f values are shown in Table A in the Supporting Information. While pure samples of *cis*-dihydrodiols **1d** and **2e** could not be obtained by chromatographic separation of relevant isomeric mixtures, *cis*-dihydrodiol **1d** was synthesized by substitution of the iodine atom in *cis*-dihydrodiol **1g**. By a slight modification—through the addition of triethylamine—in the procedure used earlier^[33] for the monocyclic *cis*-dihydrodiol series [Bu₃SnCN, Pd(PPh₃)₄ in THF], *cis*-dihydrodiol **1d** was formed from *cis*-dihydrodiol **1g** in 76% yield.

The formation of the corresponding diastereoisomeric boronate esters from (*R*)- and (*S*)-2-(1-methoxyethyl)benzeneboronic acid followed by ¹H NMR analysis of the diastereoisomeric composition^[32–35] indicated that in all cases the *ee* values were >98%.

Computational details: All excited-state calculations in our computations were performed on the basis of the ground-state geometries of single molecules, with the use of a Gaussian program package.^[40] Rotatory strengths were calculated with the use of both length and velocity representations. In this study, the differences between the lengths and velocities of calculated values of rotatory strengths were quite small, and for this reason only length representations were taken into account. The CD spectra were simulated by overlapping Gaussian functions for each transition by the procedure described by Diedrich and Grimme.^[26]

Our computational analyses were performed by a classical methodology. This includes as the first step the conformational analysis for the *cis*-dihydrodiol, then the geometry optimisation of each low-energy conformer, calculation of the rotatory strength and optical rotation for individual stable conformers and, as the last step, comparison between the Boltzmann-averaged calculated CD spectra and optical rotation with the experimental data.

Conformational analyses and geometry calculations were performed at the B3LYP/6-311++G(D,P) level. The fully optimized **P** and **M** conformers of **1f**, in which selected hydrogen atoms were replaced by the corresponding substituents, were taken as starting points for conformational analyses. In some cases geometry calculations were performed at the B2PLYP/6-311++G(D,P) level, but because of the similarity between results obtained with the use of B2PLYP and B3LYP hybrids, only the latter were taken into consideration (see the Supporting Information). For optimized structures, frequency calculations were carried out at the B3LYP/6-311++G(D,P) level of theory to confirm that the conformers were stable. For all conformers with relative energies ranging from 0.0 to 2.0 kcal mol⁻¹, percentage populations were calculated for each compound on the basis of the ΔE and ΔG values, with use of Boltzmann statistics and $T=298$ K. Because of their similarity, only ΔE values were taken into further consideration.

To test which combination of functional/basis set performs best in the case of calculations of the CD spectra of substituted naphthalene *cis*-dihydrodiols, the B2PLYP hybrid functionals were employed in combination with different basis sets (see the Supporting Information). The basis sets differ from relatively small to enhanced, with or without the diffuse functions. The best combination was B2PLYP/6-311++G(2D,2P), and

this was used for calculating the CD spectra. Additionally, the CD spectra were calculated with the use of B3LYP and mPW1PW91 hybrid functionals and 6-311++G(2D,2P) basis set and with the use of the B2PLYP/CC-pVTZ method. The computed oscillator strengths and rotatory strengths were converted into the UV and CD spectra by broadening to Gaussian shape absorption curves. The calculated spectra were blue-shifted by ca. 10–15 nm in relation to the experimental ones when the B2PLYP/6-311++G(2D,2P) and B2PLYP/CC-pVTZ methods were used. In contrast, the CD spectra calculated with the mPW1PW91 and B3LYP hybrid functionals and 6-311++G(2D,2P) basis set were underestimated by 10 and 5 nm, respectively.

Although each experimental spectrum was reproduced well by either B3LYP or mPW1PW91 hybrid functionals, in conjunction with the basis sets augmented with diffuse functions, still better overall agreement was obtained with the use of the B2PLYP hybrid functional and 6-311++G(2D,2P) basis set. It is well known that the hybrid functionals including non-local correlation effects generally provide results close to, or even better than, those obtained with the widely used B3LYP method both for the ground and for the excited states. The double-hybrid functionals feature a large amount of HF exchange ($\approx 50\%$), so the self-interaction and related errors are considerably reduced in relation to local GGAs and normal hybrid functionals (20% HF exchange).^[31] The ORs were calculated at the B3LYP/6-311++G(2D,2P) and B3LYP/Aug-CC-pVTZ levels for selected *cis*-dihydrodiols. Because of similar values of the calculated ORs and longer calculation times required for the B3LYP/Aug-CC-pVTZ method, the ORs for other *cis*-dihydrodiol molecules were calculated only at the B3LYP/6-311++G(2D,2P) level.

No correlation for the medium dielectric constant was implemented. For a detailed discussion see refs. [32] and [34].

Acknowledgements

This work was supported by grant No. N N204056335 from the Ministry of Science and Higher Education (Poland), an EU Marie Curie Host Fellowship for Transfer of Knowledge, Novocat, Project No.29846 (to M.K.) and a Science Foundation Ireland Grant No. 04/IN3/B581 (to N.D.S.). All calculations were performed at Poznań Supercomputing Centre, Poland.

- [1] D. T. Gibson, J. R. Koch, R. E. Kallio, *Biochemistry* **1968**, *7*, 2653–2661.
- [2] D. A. Widdowson, D. W. Ribbons, *Janssen Chim. Acta* **1990**, *8*, 3–9.
- [3] H. J. Carless, *Tetrahedron: Asymmetry* **1992**, *3*, 795–826.
- [4] G. N. Sheldrake in *Chirality in Industry* (Eds.: A. N. Collins, G. N. Sheldrake, J. Crosby), Wiley, New York, **1992**, Chapter 6, pp. 128–166.
- [5] S. M. Brown, T. Hudlicky, in *Organic Synthesis: Theory and Applications*, JAI Press, Greenwich, **1993**, pp. 113–176.
- [6] S. M. Resnick, K. Lee, D. T. Gibson, *J. Ind. Microbiol.* **1996**, *17*, 438–457.
- [7] D. R. Boyd, G. N. Sheldrake, *Nat. Prod. Rep.* **1998**, *15*, 309–324.
- [8] T. Hudlicky, D. Gonzalez, D. T. Gibson, *Aldrichimica Acta* **1999**, *32*, 35–62.
- [9] D. T. Gibson, R. E. Parales, *Curr. Opin. Biotechnol.* **2000**, *11*, 236–243.
- [10] D. R. Boyd, N. D. Sharma, C. C. R. Allen, *Curr. Opin. Biotechnol.* **2001**, *12*, 564–573.
- [11] R. A. Johnson, *Org. React.* **2004**, *63*, 117–264.
- [12] D. R. Boyd, T. Bugg, *Org. Biomol. Chem.* **2006**, *4*, 181–192.
- [13] D. R. Boyd, N. D. Sharma, G. P. Coen, F. Hempenstall, V. Ljubez, J. F. Malone, C. C. R. Allen, J. T. G. Hamilton, *Org. Biomol. Chem.* **2008**, 3957–3966.
- [14] T. Hudlicky, M. A. Endoma, G. Butora, *Tetrahedron: Asymmetry* **1996**, *7*, 61–68.
- [15] G. M. Whited, J. C. Downie, T. Hudlicky, S. F. Fearnley, T. C. Dudding, H. F. Olivo, D. Parker, *Bioorg. Med. Chem.* **1994**, *2*, 727–734.
- [16] M. E. Deluca, T. Hudlicky, *Tetrahedron Lett.* **1990**, *31*, 13–16.
- [17] M. Jeffrey, H. J. C. Yeh, D. M. Jerina, T. R. Patel, J. F. Davey, D. T. Gibson, *Biochemistry* **1975**, *14*, 575–584.
- [18] G. Bestetti, G. Bianchi, A. Bosetti, P. Di Gennaro, E. Galli, B. Leoni, F. Pelizzoni, G. Sello, *Appl. Microbiol. Biotechnol.* **1995**, *44*, 306–313.
- [19] C. Brilon, W. Beckmann, H.-J. Knackmuss, *Appl. Environ. Microbiol.* **1981**, *42*, 44–55.
- [20] Selected articles: a) D. Marchesan, S. Coriani, C. Forzato, P. Nitti, G. Pitacco, K. Ruud, *J. Phys. Chem. A* **2005**, *109*, 1449–1453; b) D. M. McCann, P. J. Stephens, J. R. Cheeseman, *J. Org. Chem.* **2004**, *69*, 8709–8717; c) A. Lattanzi, R. G. Viglione, A. Scettri, R. Zanasi, *J. Phys. Chem. A* **2004**, *108*, 10749–10753; d) K. Ruud, P. J. Stephens, F. J. Devlin, P. R. Taylor, J. R. Cheeseman, M. J. Frisch, *Chem. Phys. Lett.* **2003**, *373*, 606–614; e) P. J. Stephens, F. J. Devlin, J. R. Cheeseman, M. J. Frisch, O. Bortolini, P. Besse, *Chirality* **2003**, *15*, S57–S64; f) P. J. Stephens, F. J. Devlin, J. R. Cheeseman, M. J. Frisch, *J. Phys. Chem. A* **2001**, *105*, 5356–5371; g) S. Grimme, *Chem. Phys. Lett.* **2001**, *339*, 380–388.
- [21] a) H. D. Flack, G. Bernardinelli, *Chirality* **2008**, *20*, 681–690; b) I. Weissbuch, L. Leiserowitz, M. Lahav, *Chirality* **2008**, *20*, 736–748; c) E. L. Eliel, S. H. Wilen, L. N. Mander, *Stereochemistry of Organic Compounds*, Wiley, New York, **1994**.
- [22] See for example: a) P. L. Polavarapu, *Chirality* **2008**, *20*, 664–672; b) P. J. Stephens, J.-J. Pan, F. J. Devlin, M. Urbanová, O. Julínek, J. Hájiček, *Chirality* **2008**, *20*, 454–470; c) P. J. Stephens, D. M. McCann, F. J. Devlin, J. R. Cheeseman, M. J. Frisch, *J. Am. Chem. Soc.* **2004**, *126*, 7514–7521; d) P. J. Stephens, F. J. Devlin, F. Gasparini, A. Ciogli, D. Spinelli, B. Cosimelli, *J. Org. Chem.* **2007**, *72*, 4707–4715; e) D. M. McCann, P. J. Stephens, *J. Org. Chem.* **2006**, *71*, 6074–6098; f) T. D. Crawford, M. L. Abrams, T. D. Crawford, *J. Phys. Chem. A* **2006**, *110*, 7649–7654.
- [23] a) T. D. Crawford, M. C. Tam, M. L. Abrams, *J. Phys. Chem. A* **2007**, *111*, 12057–12068; b) T. D. Crawford, *Theor. Chem. Acc.* **2006**, *115*, 227–245; c) M. Pecul, K. Ruud, *Adv. Quantum Chem.* **2005**, *50*, 185–212.
- [24] a) K. Burke, J. Werschnik, E. K. U. Gross, *J. Chem. Phys.* **2005**, *123*, 062206; b) T. Mori, Y. Inoue, S. Grimme, *J. Org. Chem.* **2006**, *71*, 9797–9806; c) T. D. Crawford, P. J. Stephens, *J. Phys. Chem. A* **2008**, *112*, 1339–1345; d) M. Dierksen, S. Grimme, *J. Chem. Phys.* **2006**, *124*, 174301; e) J. Autschbach, T. Ziegler, S. J. A. van Gisbergen, E. J. Baerends, *J. Chem. Phys.* **2002**, *116*, 6930–6940.
- [25] Y. Zhao, D. G. Truhlar, *Acc. Chem. Res.* **2008**, *41*, 157–167.
- [26] C. Diedrich, S. Grimme, *J. Phys. Chem. A* **2003**, *107*, 2524–2539.
- [27] S. Grimme, M. Steinmetz, M. Korth, *J. Chem. Theory Comput.* **2007**, *3*, 42–45.
- [28] See for example: a) E. J. Baerends, O. V. Gritsenko, *J. Chem. Phys.* **2005**, *123*, 062202; b) A. Görling, *J. Chem. Phys.* **2005**, *123*, 062203; c) P. Mori-Sánchez, Q. Wu, W. Yang, *J. Chem. Phys.* **2005**, *123*, 062204; d) J. P. Perdew, A. Ruzsinszky, J. Tao, V. N. Staroverov, G. E. Scuseria, G. I. Csonka, *J. Chem. Phys.* **2005**, *123*, 062201; e) S. Grimme, *J. Comput. Chem.* **2006**, *27*, 1787–1799; f) S. Grimme, J. Antony, T. Schwabe, C. Mück-Lichtenfeld, *Org. Biomol. Chem.* **2007**, *5*, 741–758.
- [29] D. Jacquemin, E. A. Perpète, G. E. Scuseria, I. Ciofini, C. Adamo, *J. Chem. Theory Comput.* **2008**, *4*, 123–135.
- [30] T. Schwabe, S. Grimme, *Phys. Chem. Chem. Phys.* **2006**, *8*, 4398–4401.
- [31] a) S. Grimme, F. Neese, *J. Chem. Phys.* **2007**, *127*, 154116; b) S. Grimme, *J. Chem. Phys.* **2006**, *124*, 034108.
- [32] J. Gawronski, M. Kwit, D. R. Boyd, A. Drake, J. F. Malone, N. D. Sharma, *J. Am. Chem. Soc.* **2005**, *127*, 4308–4319.
- [33] D. R. Boyd, N. D. Sharma, G. N. Coen, P. Gray, J. F. Malone, J. Gawronski, *Chem. Eur. J.* **2007**, *13*, 5804–5811.
- [34] M. Kwit, N. D. Sharma, D. R. Boyd, J. Gawronski, *Chem. Eur. J.* **2007**, *13*, 5812–5821.
- [35] M. Kwit, N. D. Sharma, D. R. Boyd, J. Gawronski, *Chirality* **2008**, *20*, 609–620.

- [36] a) P. Crabbé, W. Klyne, *Tetrahedron* **1967**, *23*, 3449–3503; b) P. Crabbé, A. Cruz, J. Iriarte, *Can. J. Chem.* **1968**, *46*, 349–363; c) N. A. R. Hatam, D. A. Whiting, *J. Chem. Soc. Perkin Trans. 1* **1982**, 461–465; d) G. Quinkert, M. Del-Grosso, A. Döring, W. Döring, R. I. Schenkel, M. Bauch, G. T. Dambacher, J. W. Bats, G. Zimmermann, G. Dürner, *Helv. Chim. Acta* **1995**, *78*, 1345–1391.
- [37] T. Linker, F. Rebien, G. Tóth, A. Simon, J. Kraus, G. Bringmann, *Chem. Eur. J.* **1998**, *4*, 1944–1951.
- [38] A. H. W. Aten, J. C. Kapteyn, *J. Phys. Chem.* **1979**, *83*, 2178.
- [39] P. Crabbé, *Chem. Ind. (London)* **1969**, 917–918.
- [40] Gaussian 03 (Revision D.0), M. A. Robb, J. R. Cheeseman, J. A. Montgomery, Jr., T. Vreven, K. N. Kudin, J. C. Burant, J. M. Millam, S. S. Iyengar, J. Tomasi, V. Barone, B. Mennucci, M. Cossi, G. Scalmani, N. Rega, G. A. Petersson, H. Nakatsuji, M. Hada, M. Ehara, K. Toyota, R. Fukuda, J. Hasegawa, M. Ishida, T. Nakajima, Y. Honda, O. Kitao, H. Nakai, M. Klene, X. Li, J. E. Knox, H. P. Hratchian, J. B. Cross, V. Bakken, C. Adamo, J. Jaramillo, R. Gomperts, R. E. Stratmann, O. Yazyev, A. J. Austin, R. Cammi, C. Pomelli, J. W. Ochterski, P. Y. Ayala, K. Morokuma, G. A. Voth, P. Salvador, J. J. Dannenberg, V. G. Zakrzewski, S. Dapprich, A. D. Daniels, M. C. Strain, O. Farkas, D. K. Malick, A. D. Rabuck, K. Raghavachari, J. B. Foresman, J. V. Ortiz, Q. Cui, A. G. Baboul, S. Clifford, J. Cioslowski, B. B. Stefanov, G. Liu, A. Liashenko, P. Piskorz, I. Komaromi, R. L. Martin, D. J. Fox, T. Keith, M. A. Al-Laham, C. Y. Peng, A. Nanayakkara, M. Challacombe, P. M. W. Gill, B. Johnson, W. Chen, M. W. Wong, C. Gonzalez, J. A. Pople, Gaussian, Inc., Wallingford CT, **2004**
- [41] A. Klapars, S. L. Buchwald, *J. Am. Chem. Soc.* **2002**, *124*, 14844–14845.
- [42] D. R. Boyd, N. D. Sharma, B. Byrne, M. V. Hand, J. F. Malone, G. N. Sheldrake, J. Blacker, H. Dalton, *J. Chem. Soc. Perkin Trans. 1* **1998**, 1935–1943.

Received: August 14, 2008
Published online: November 12, 2008